Non-Invasive Estimation of the Activation Sequence in the Atria during Sinus Rhythm and Atrial Tachyarrhythmia

Jorge Pedrón-Torrecilla[1], Andreu M Climent[1], Alejandro Liberos[1], Esther Pérez-David[2], José Millet[1], Felipe Atienza[2], Maria S Guillem[1]

[1]Bio-ITACA, Universitat Politècnica de València, Valencia, Spain
[2]Hospital General Universitario Gregorio Marañón, Madrid, Spain

Abstract

Ablation procedures have become one of the most efficient treatments for termination of atrial arrhythmias. The aim of the present study is the evaluation of the potential use of noninvasive imaging as a clinical tool for the identification of atrial tachycardia origin prior to an ablation procedure. Simultaneous 67-lead body surface potential recordings and 15 intracardiac electrograms (EGM) were obtained for one patient during sinus rhythm and pacing the left superior pulmonary vein. 3D heart and torso geometries were obtained by using computed axial tomography images. Epicardial activation sequences were computed by solving the inverse problem of the electrocardiology. Reconstructed activation sequences were consistent with recorded EGMs. Measured and estimated activation time differences between right and left atria were 93 ms and 102 ms during sinus rhythm respectively and 49 ms and 71 ms respectively during left atrial pacing.

1. Introduction

Atrial arrhythmias are great of concern in clinical electrocardiology. Atrial fibrillation and other arrhythmias can be maintained by a small tissue area [1]. Ablation procedures have become one of the most efficient treatments since isolation of these regions usually results in termination the arrhythmia.

In the clinical setting, identification of ablation targets is achieved by electroanatomical mapping. Electro-anatomical mapping presents significant limitations in the characterization of AF processes resulting from a sequential acquisition of mapping points under a non-stationary activation. Prior knowledge of source location may help ablation planning and reduce the procedure time. The aim of this study is to evaluate the noninvasive electrocardiographic imaging technique as a clinical tool for the identification of the origin of atrial tachycardias. In this study, simulated and real body surface potential mapping recordings were used to reconstruct the epicardial activity in the atria. Results were validated by using simultaneous intracardiac recordings.

2. Methods

Methodology section is divided as follows: (1) technical details of the inverse problem resolution are summarized, (2) mathematical models used to validate the methodology are described and, (3) a clinical case study used to illustrate the performance of the technique is described.

2.1. Inverse problem resolution

In order to obtain the potentials on the heart surface from the potentials recorded non-invasively from the torso surface of the patient, we solved the inverse problem of the electrocardiography by using the Boundary Element Method (BEM).

According to the BEM formulation [2-5], potentials on the surface of the torso can be computed from potentials on the heart surface by using (1)-(3):

$$A_1 x = b \qquad (1)$$

$$A_1 = \begin{pmatrix} D_{HH(nxn)} & G_{HH(nxn)} \\ D_{BH(mxn)} & G_{BH(mxn)} \end{pmatrix}, \quad X = \begin{pmatrix} \Phi_H \\ \Gamma_H \end{pmatrix},$$

$$b = \begin{pmatrix} -D_{HB(nxm)}\Phi_B \\ -D_{BB(mxm)}\Phi_B \end{pmatrix} \qquad (2)$$

$$\Phi_B = A\Phi_H = \left(D_{BB} - G_{BH}G_{HH}^{-1}D_{HB}\right)^{-1} \cdot \left(G_{BH}G_{HH}^{-1}D_{HH} - D_{BH}\right)\Phi_H \qquad (3)$$

where Φ_H is the potential on the surface of the heart, Φ_B is the potential on the surface of the torso, Γ_H is the potential gradient of the heart, D_{XY} is the potential transfer matrix from point Y to point X and G_{XY} is the potential gradient transfer matrix from point Y to point X.

The inverse problem can be solved by computing the inverse of matrix A (A^{-1}). However, A is ill-conditioned

and, in order to overcome the ill-conditioned nature of *A*, the system needs to be regularized. This regularization can be accomplished by using Tikhonov's method, which consists of a minimization problem (4):

$$\min_{x\in E^n}\left\{\left\|A\Phi_H-\Phi_B\right\|^2+t\left\|B\Phi_H\right\|^2\right\} \quad (4)$$

where *t* is a regularization parameter that can be obtained with the L-curve method and *B* is the spatial regularization matrix which is the identity matrix (zero-order). Therefore, the inverse problem can be solved by using the expression (5):

$$\Phi_H(t)=\left(A^TA+tB^TB\right)^{-1}A^T\Phi_B \quad (5)$$

Unipolar electrograms were then computed by applying (5) on the beats previously computed for each electrocardiographic lead.

In order to localize the origin of the atrial P-waves and reconstruct the activation sequence, electrograms (EGMs) were analyzed in terms of their activation times. Activation times of unipolar electrograms were computed as those instants with a maximum –dV/dt and activation times of bipolar electrograms were computed as those instants with maximum amplitude.

2.2. Inverse problem validation

Inverse problem was validated by using a realistic mathematical model. Specifically, sinus rhythm propagation pattern was calculated in a three-dimensional structure of human atria of approximately 12.5x9 cm [6] with 577264 nodes. Briefly, the action potential of each node was mathematically constructed to include ionic currents, ionic pumps and exchangers, and processes regulating intracellular concentration changes of Na^+, K^+ and Ca^{2+} [7]. Neighboring cells were coupled by a coupling conductance *g*, which was adjusted to obtain a realistic conduction velocity. The evolution of the transmembrane voltage of each cell (i.e. V_i for the i-th cell) V_i, was controlled by the following first-order, time-dependent ordinary differential equation:

$$\frac{dV_i}{dt}=-\frac{1}{C_m}\left(I_{total,i}+\sum\nolimits_j g_{i,j}\left\{V_i-V_j\right\}\right) \quad (1)$$

where $I_{total,i}$ summarizes the contribution of all transmembrane currents [7], C_m is the transmembrane capacitance, and $g_{i,j}$ is the conductance between neighbor cells *i* and *j*.

A simulation of a sinus rhythm propagation was created by applying a 5ms stimulus from the region of the sinus node. Mathematical computations were performed by using an adaptive time-step solver on a Graphical Processing Unit [8]. Simulated EGMs (i.e. 5697 signals) were calculated by using transmembrane potentials generated by the cellular mathematical model [6]:

$$EGM=\sum_{\vec{r}}\left(\frac{\vec{r}}{r^3}\right)\cdot\vec{\nabla}V_m \quad (6)$$

where $\vec{r}$ is the distance vector between the measuring point and a point in the tissue domain (*r* is the distance scalar), $\vec{\nabla}$ denotes the gradient operator and V_m is the transmembrane potential. Body surface potential mapping signals were computed from EGMs by solving the forward problem [2-5]. Specifically, ECGs on a torso model with 771 nodes and 1538 faces were estimated [9,10].

Simulated ECGs were used to reconstruct epicardial electrograms by means of the inverse problem resolution described in section 2.1. Finally, simulated and reconstructed electrograms were compared in order to validate the identification of the origin of the activation sequence from noninvasive signals.

2.3. Clinical case study

The included case study was a patient admitted for ablation of drug-refractory paroxysmal atrial fibrillation. The subject was in sinus rhythm at the beginning of the intervention. During the electrophysiological study, 15 bipolar EGMs and a 64-channel BSPM recording were registered simultaneously. In order to illustrate the presented methodology recordings during two propagation patterns are used; (1) during sinus rhythm (SR) and (2) during an atrial tachycardia generated by pacing from the left superior pulmonary vein (LSPV).

Prior to the intervention, computer axial tomography (CAT) images with a resolution of 0,5 mm were acquired to build the 3D atrial and torso models. Specifically, heart and torso conductive volumes were segmented from CAT images and isotropic and homogeneous conductivities of 0.6 S/m and 0.2 S/m respectively. Both surfaces were tessellated into flat triangles, using 3615 nodes and 7222 faces for the atrial surface and 2689 nodes and 5374 faces for the torso surface.

During the entire ablation procedure, patients wore a custom-made adjustable vest with 64 electrodes covering the entire torso surface (Figure 1) plus 3 electrodes used for recording the limb leads. The vest included recording electrodes in the anterior (N=28), posterior (N=34) and lateral sides (N=2) of the torso. Signals were acquired at a sampling rate of 2048 Hz, with a resolution of 1 μV and a bandwidth of 500 Hz. Before acquisition, signal quality of all leads was visually inspected and ECGs were stored for off-line processing [11]. Additionally, 15 bipolar EGMs were simultaneously recorded by using a standard tetrapolar catheter in the right atrial (RA) appendage; 2) a deflectable 4 mm mapping catheter (Marinr, Medtronic Inc., Minneapolis, USA) in the distal coronary sinus (CS); 3) a decapolar circular mapping Lasso catheter (Biosense-Webster, Diamond Bar, CA, USA) used to map the left

superior pulmonary vein (LSPV); and 4) a Navistar catheter (3.5 mm tip, 2-5-2 interelectrode distance, Thermo-Cool, Biosense-Webster, Diamond Bar, CA, USA) used to stimulate. EGM signals were acquired at a sampling rate of 977 Hz, with a resolution of 1 μV.

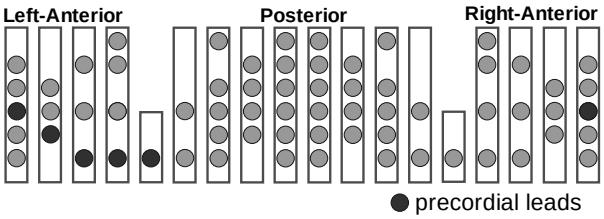

Figure 1. Electrode position in our BSPM system. Black circles correspond to the approximate location of precordial, right and left arm leads.

ECG signals were processed using Matlab 2010 (The Mathworks Inc, The Netherlands). First, the baseline was estimated by filtering with a butterworth 10th order low-pass filter with a cut-off frequency of 0.8 Hz after decimation to a sampling frequency of 51.2 Hz. Baseline was interpolated to 2048 Hz and subtracted to the original recording. Then, ECG signals were filtered with a 10th order, low-pass Butterworth filter with a cut-off frequency of 70 Hz. Power spectral density of all signals was computed by using a Welch periodogram with a Hamming window of 8 seconds and 50% overlap. Leads presenting more than 0.5% of their spectral content at 50 Hz were filtered with a 2nd order IIR notch filter centered at 50 Hz. All leads were visually inspected after filtering and leads with noticeable noise or very low amplitude were excluded from further analysis.

Two representative P-waves were used for noninvasive estimation of intracardial EGMs by using the methods described above (i.e. one during sinus rhythm and one during LSPV stimulation). The reconstructed atrial propagation pattern was compared with the 15 simultaneously recorded intracardiac catheter signals.

3. Results

3.1. Inverse problem validation

In Fig. 2A, the isochronal map of the reconstructed activation sequence from the simulated data is depicted.

The solution of the inverse problem showed an activation sequence starting at the sinus node that propagates to the right and left atria across the Bachmann's bundle. The stimulation node was detected with an error of 7 mm. In Fig. 2B three EGMs from the RA, CS and LSPV are depicted which are consistent with the reconstructed activation sequence. Difference between the activation times in atria and those computed after inverse problem solution was 2.19 ± 10.58 ms.

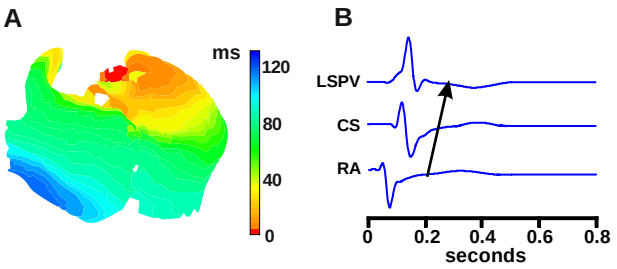

Figure 2. (A) Activation sequence obtained by solving the inverse problem in the mathematical model during sinus rhythm. (B) Simulated unipolar EGMs obtained at the left superior pulmonary vein (LSPV), coronary sinus (CS) and right atrium (RA).

3.2. Clinical case study

The reconstruction of the epicardial activation sequence during sinus rhythm allowed the identification of a propagation pattern from the right to the left atrium (Fig. 3A). Recorded EGMs were consistent with the computed activation sequence: the activation can be first observed in the RA catheter, followed by the CS and the LSPV (Fig. 3B). EGMs showed a difference between the activation of the RA and LSPV of 93 ms. Noninvasively computed activation times of the RA and the LA showed a maximum time difference of 102 ms.

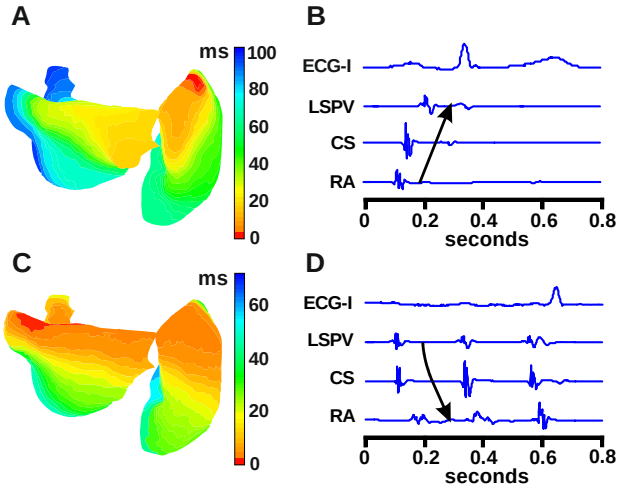

Figure 3. Noninvasive reconstruction of activation sequences during (A) sinus rhythm and (C) left atrial stimulation. (B, D) Lead I on the standard ECG and bipolar EGMs from the left superior pulmonary vein (LSPV), coronary sinus (CS) and right atrium (RA).

When the LSPV was paced, EGMs showed an earlier activation in the LSPV followed by an activation in the the CS and a final activation of the RA (Fig. 3D). The difference in the activation time between LSPV and RA EGMs was 49 ms. Inverse reconstruction of the epicardial propagation pattern showed one wavefront starting at the

LSPV (Fig. 3C) and a depolarization of the most distal part of the RA taking place 71 ms after the stimulation.

4. Discussion and conclusion

In the present study, noninvasive recordings and the solution of the inverse problem of the electrocardiography were used to estimate the epicardial activation sequence from a patient under sinus rhythm and atrial tachycardia generated by pacing at the left superior pulmonary vein. Experimental results were consistent with simultaneously recorded intracardiac EGMs and measured and inverse-computed activation times were comparable.

In addition, mathematical simulations were used to quantify the accuracy of reconstructed activation sequences. The origin of electrical activation was could be determined within a few mm and activation times were reconstructed with an almost negligible error. By using this detailed ionic model of the atria, different clinical scenarios could be simulated (i.e. sinus rhythm, atrial tachycardia, atrial flutter or atrial fibrillation) and used to evaluate the accuracy of the inverse problem solution to estimate more complex propagation patterns and to clarify the relation between epicardial propagation patterns and its representation on the torso [11].

The methods described in this work may be useful for planning an ablation procedure. During the last years, different groups have developed and tested the methodology to noninvasively reconstruct the epicardial activation sequence during atrial tachycardias [12, 13], atrial flutter and atrial fibrillation [14]. Although cardiac mapping can be used to detect stable foci in the atria or to characterize a re-entrant pattern during atrial flutter, location of atrial sources during fibrillation is more complicated since contact mapping is performed sequentially. A non-invasive reconstruction of the atrial activation sequence based on the recording of multiple simultaneous ECGs may overcome this limitation.

Noninvasive mapping has demonstrated to be a promising tool in the diagnosis of atrial arrhythmias and may help in planning ablation procedures.

Acknowledgements

This work was partially supported by Spanish Ministry of Economy (TEC2009-13939), Universitat Politècnica de València (PAID-2009-2012) and by the Generalitat Valenciana (AP-145/10 and PROMETEO2010/093).

References

[1] Haïssaguerre M, Jaïs P, Shah D, Takahashi A, Hocino M, Quiniou G, Garrigue S, Le Mouroux A, Le Métayer P, Clémenty J. Spontaneous initiation of atrial fibrillation by ectopic beats originating in the pulmonary veins. N Engl J Med 1998;339(10):659-66.

[2] Stenroos M. The transfer matrix for epicardial potential in a piece-wise homogeneous thorax model: boundary element formulation. Physics in Medicine and Biology 2009;54:5443-55.

[3] Horácek B.M, Clements J.C. The Inverse Problem of Electrocardiography: A Solution in Terms of Single- and Double-Layer Sources on the Epicardial Surface. Mathematical Biosciences 1997;144:119-54.

[4] De Munck J.C. A linear Discretization of the Volume Conductor Boundary Integral Equation Using Analytically Integral Elements. IEEE Trans on Biomedical Engineering 1992;39(9):986-90.

[5] Cowper G.R. Gaussian Quadrature Formulas For Triangles. Int. J. Num. Meth. Eng 1972;7(3):405-8.

[6] Harrild D.M, Henriquez C.S. A computer model of normal conduction in the human atria. Circ Res 2000;87:E25-E36.

[7] Courtemanche M, Ramirez R.J, Nattel S. Ionic mechanisms underlying human atrial action potential properties: Insights from a mathematical model. Am J Physiol -Heart Circul Physiol 1998;275:H301-H321.

[8] Garcia V.M, Liberos A, Climent A.M, Vidal A, Mollet J, González A. An adaptive step size GPU ODE solver for simulating the electric cardiac activity. CinC 2011;38:233-6.

[9] MacLeod R.S, Johnson C.R, and Ershler P.R. Construction of an Inhomogeneous Model of the Human Torso for Use in Computational Electrocardiography. 13th Ann Int Conf, IEEE Eng Med and Biol Soc 1991;1991:688-9.

[10] Pedrón-Torrecilla J, Climent A.M, Millet J, Berné P, Brugada J, Brugada R, Guillem M.S. Characteristics of inverse-computed epicardial electrograms of Brugada sindrome patients. 33rd Ann Int Conf IEEE Eng Med Biol Soc 2011;2011:235-8.

[11] Guillem M.S, Climent A.M, Castells F, Husser D, Millet J, Arya A, Piorkowski C, Bollmann A. Noninvasive Mapping of Human Atrial Fibrillation. JCE 2009;20(5):507-13.

[12] Ramanathan C, Ghanem RN, Jia P, Ryu K, Rudy Y. Noninvasive electrocardiographic imaging for cardiac electrophysiology and arrhythmia. Nat Med 2004;10:422-8.

[13] Roten L, Pedersen M, Pasacale P, Shah A, Eliautou S, Scherr D, Sacher F, Haïssaguerre M. Noninvasive Electrocardiographic Mapping for Prediction of Tachycardia Mechanism and Origin of Atrial Tachycardia Following Bilateral Pulmonary Transplantation. J Cardiovasc Electrophysiol 2012;23(5):553-5.

[14] Cuculich P.S, Wang Y, Lindsay B.D, Faddis M.N, Schuessler R.B, Damiano Jr R.J, Li L, Rudy Y. Noninvasive characterization of epicardial activations in humans with diverse atrial fibrillation patterns. Circulation 2010;122:1364-72.

Address for correspondence.

Jorge Pedrón Torrecilla.
Universitat Politècnica de València. Ed. 8G. Bio-ITACA.
Camino de Vera s/n. CP: 46022. Valencia, Valencia, Spain.
jorpedto@upvnet.upv.com.